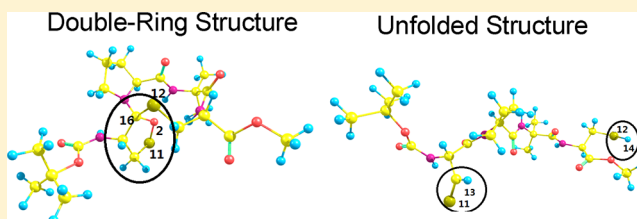


# The Folding Dynamics and Infrared Spectra of a Photocleaved Tetrapeptide Predicted by Theoretical Simulations

Tiantian Jiao, Lianghui Gao,\* Xuebo Chen, and Weihai Fang

Key Laboratory of Theoretical and Computational Photochemistry, Ministry of Education, College of Chemistry, Beijing Normal University, Beijing 100875, China

**ABSTRACT:** We present the theoretical investigation of the folding dynamics of a photocleaved tetrapeptide with a disulfide bridge by using combined semiempirical quantum-mechanical and molecular-mechanical molecular dynamics simulations and high-level CASPT2//CASSCF/Amber calculations. We find that in acetonitrile solvent, aside from the recombination of the sulfur biradicals, the peptide can refold to a double sulfur-heterocyclic ring structure or a fully opened structure. The radical bicyclization reaction and the intramolecular hydrogen transfer are responsible for the low recombination rate of the cysteinyl radicals, respectively. On the other hand, in methanol solvent, the formation of the solvent cages around the sulfur radicals reduces the possibility of the close contact of the radicals. The calculated infrared spectra of the amide I mode corresponding to the conformation changes of the peptide can well explain the experimental observation.



## INTRODUCTION

How the peptides or proteins fold to their native states is a challenging question in biological research.<sup>1</sup> To investigate the dynamic aspects of the folding processes requires a triggering event that can initiate the unfolded conformation. In the past few years, a novel ultrafast phototrigger technique has been developed.<sup>2–4</sup> The idea is to synthesize a disulfide bridged cyclic peptide. Since the disulfide bridge is a weak covalent bond, it can be easily cleaved by ultraviolet (UV) light and generate two S radicals, thus making it possible to trigger peptide folding on short time scales. The disulfide bond is also an important inert building block commonly existing in 80% of the proteins in the Protein Data Bank.<sup>5</sup> It governs the stability and the function of the proteins. The mechanism of the photocleavage and the subsequent (un)folding dynamics are currently under active theoretical and experimental investigations.

A number of experimental approaches have been developed for the real-time observation of the peptide or protein (un)folding processes, such as infrared absorption,<sup>6</sup> resonant Raman scattering,<sup>7</sup> circular dichroism,<sup>8</sup> and so on. These techniques are able to follow the structure changes concerning the protein folding or unfolding. For example, transient two-dimensional infrared (2D-IR) spectroscopy of a disulfide bridged cyclic tetrapeptide [cyclo(Boc-Cys-Pro-Aib-Cys-OMe), see Figure 1a for the molecular structure] reveals that the cysteinyl radicals generated by photocleavage (300 nm UV light) diffuse on an unusual time scale from 100 ps to 10  $\mu$ s before their recombination.<sup>9,10</sup> In contrast, Volk and Hochstrasser reported that an aryl disulfide-linked artificial  $\alpha$ -helical polypeptide with 17 amino acids had a much higher recombination rate.<sup>3</sup> The mechanisms governing the photocleavage and folding dynamics on the atomic and electronic

structure levels cannot be gained simply from experiments. Detailed insight into the mechanisms needs elucidations from the computer simulations.<sup>9,11,12</sup> For example, the non-equilibrium classical molecular dynamics (MD) indicated that the strain in the cyclic tetrapeptide backbone may keep the two S radicals apart and prevents recombination.<sup>9</sup> However, the classical MD is unable to describe the bond breaking and formation. Nieber et al.<sup>12</sup> performed linked non-adiabatic ab initio MD and classical MD simulations for the tetrapeptide in acetonitrile solvent. They predicted that the intramolecular hydrogen transfer may be responsible for the low recombination rate of the S radicals. Recently, we reported the theoretical investigation for the tetrapeptide in methanol solvent by using the combined semiempirical quantum mechanical and molecular mechanical (QM/MM) MD simulations. Our results showed that the formation of the solvent cages around the sulfur radicals reduced the possibility of the close contact of the radicals. So far, the mechanisms governing the unfolding/refolding dynamics in various solvents are still ambiguous and need to be clarified. The theoretical spectroscopy corresponding to the conformational changes of the peptides is also mandatory for the understanding of the experimental spectra.

In this article, we present our theoretical investigations by using (QM/MM) MD simulations for a cyclic tetrapeptide in both acetonitrile and methanol solvent. We find that there are different mechanisms governing the unfolding and refolding dynamics of the peptide after the photocleavage. In acetonitrile solvent, the intramolecular hydrogen transfer and sulfur radical bicyclization reaction are responsible for the low recombination

**Received:** November 15, 2012

**Revised:** November 25, 2012

**Published:** November 26, 2012

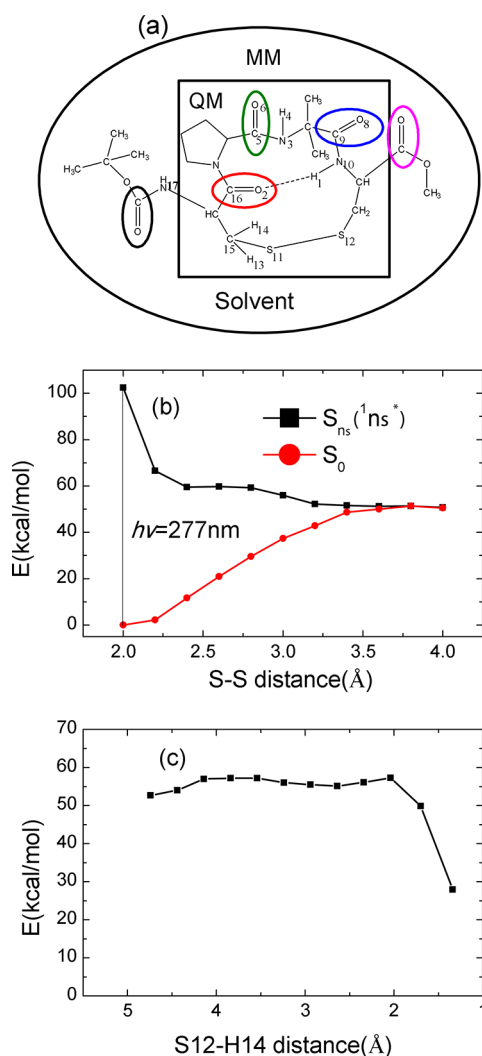


**Figure 1.** (a) Chemical structure of a disulfide bridged cyclic tetrapeptide cyclo(Boc-Cys-Pro-Aib-Cys-OMe). (b) The energy profile of the photodissociation along the S–S fission pathway. (c) The energy potential for the hydrogen H14 being transferred from C15 to S12.

rate of the cysteinyl radicals. On the other hand, in methanol solvent, once the disulfide bond breaks, the methanol molecules rapidly diffuse around the S radicals and form solvent cages which reduce the possibility of the close contact of the radicals. To have deep insight into the mechanism of the peptide refolding, we also compute the potential energy profiles of the photochemical steps by using the CASPT2//CASSCF/Amber (QM/MM) method. We further estimate the IR spectra of the amide I mode of the tetrapeptide by using the data obtained from the QM/MM MD simulations. The spectra corresponding to the conformational change can well explain the experimental observation.

## COMPUTATIONAL METHODS

Prior to the molecular dynamics simulations, we first compute the potential energy profile of the photoexcited tetrapeptide by using the high-levelled CASPT2//CASSCF/Amber (QM/MM) protocol<sup>13</sup> as given in Figure 1a. To prepare the systems, we place a disulfide bridged cyclic tetrapeptide in an acetonitrile solvent box (with 311 CH<sub>3</sub>CN molecules) or a methanol solvent box (with 384 CH<sub>3</sub>OH molecules). Then, we remove

the solvent molecules that are within 10 Å away from any given atom of the solute to avoid the improper bond formation between the solute and solvent molecules. Then, energy minimization (10 000 steps) and MD simulations up to 1 ns are performed by using the Tinker tool package<sup>14</sup> with Amber force field parameters and Gaff parameters.<sup>15</sup> The configurations generated by the classical MD simulations are then used for the subsequent QM/MM calculations. We select 45 atoms inside the  $\beta$ -turn as the QM subsystem; see Figure 1a. The remaining atoms of the solute and all solvent molecules are treated as a MM subsystem. Two hydrogen link atoms are placed between the QM and MM parts where (Boc-H)N–C(Cys) and (Cys)C–C(N–OMe) bonds are cut. We use the CASPT2//CASSCF/Amber protocol to calculate the potential energy profile of the photochemical steps. The QM calculations are performed by the GAUSSIAN<sup>16</sup> and MOLCAS programs.<sup>17</sup> The MM calculations are calculated by the Tinker tool package.<sup>14</sup> The QM and MM interactions include van der Waals and electrostatic interactions. The interfaces between the QM and MM subsystems are coded in the Tinker package and commercialized together with the MOLCAS program by Ferré et al.<sup>13</sup> A 10e/8o active space is selected for the QM calculation at the CASSCF level in the acetonitrile solvent. The orbitals and electrons in the active space are from the C16O2  $n$ ,  $\pi$ , and  $\pi^*$ , C15H14  $\sigma$  and  $\sigma^*$ , and the S–S  $n$ ,  $\sigma$ , and  $\sigma^*$ . In the methanol solvent, a 10e/9o active space is selected.<sup>11</sup> The orbitals and electrons are from the C=O  $\pi$ ,  $\pi^*$ , the C–N  $\sigma$ ,  $\sigma^*$ , and  $n$  lone pair in the peptide plane of the C6O5–N3H4, the C=O  $\pi$ ,  $\pi^*$  in the peptide plane of C9O8–N10H1, and the S–S  $\sigma$ ,  $\sigma^*$ .

The unfolding and refolding dynamics following the photocleavage of the S–S bond are simulated by using the combined semiempirical QM/MM MD simulation. In the MD simulations, the QM subsystem includes all the atoms of the solute, while the MM subsystem is composed of all of the solvent molecules. The Hamiltonian for the interactions between the QM particles is given by the PM6 method.<sup>18</sup> The configuration interaction resulting from the mixing of four microstates is used to describe characters of the S biradicals. The Amber force field with supplementation of Gaff parameters<sup>15</sup> is used to calculate the interactions between the MM atoms. The QM/MM parts interact via van der Waals and electrostatic interactions. For the electrostatic interactions, we first fit the electrostatic potential from the QM calculation and obtain the effective point charge on each QM atom. Then, we calculate the Coulomb interaction between the point charges of the QM atoms and the point charges of the MM atoms. The combined semiempirical QM/MM MD method is able to describe the formation and breaking of the chemical bonds comparing to classical MD simulations, and significantly reduce the simulation time compared with the ab initio MD simulations. The QM/MM MD simulations are performed in the NVT ( $T = 298\text{ K}$ ) ensemble with a time step of 0.2 fs using the Tinker tool packages. We first run simulations by fixing the positions of the peptide for 200 ps. Trajectories are recorded every 2 ps to obtain 100 samples. Then, each sample is simulated for 1 ns to give statistics of the unfolding or refolding events.

The partial charges obtained by fitting the electrostatic potential surface to the atom centered charges and the coordinates saved during the semiempirical QM/MM MD simulation are used to calculate the infrared spectrum. Within

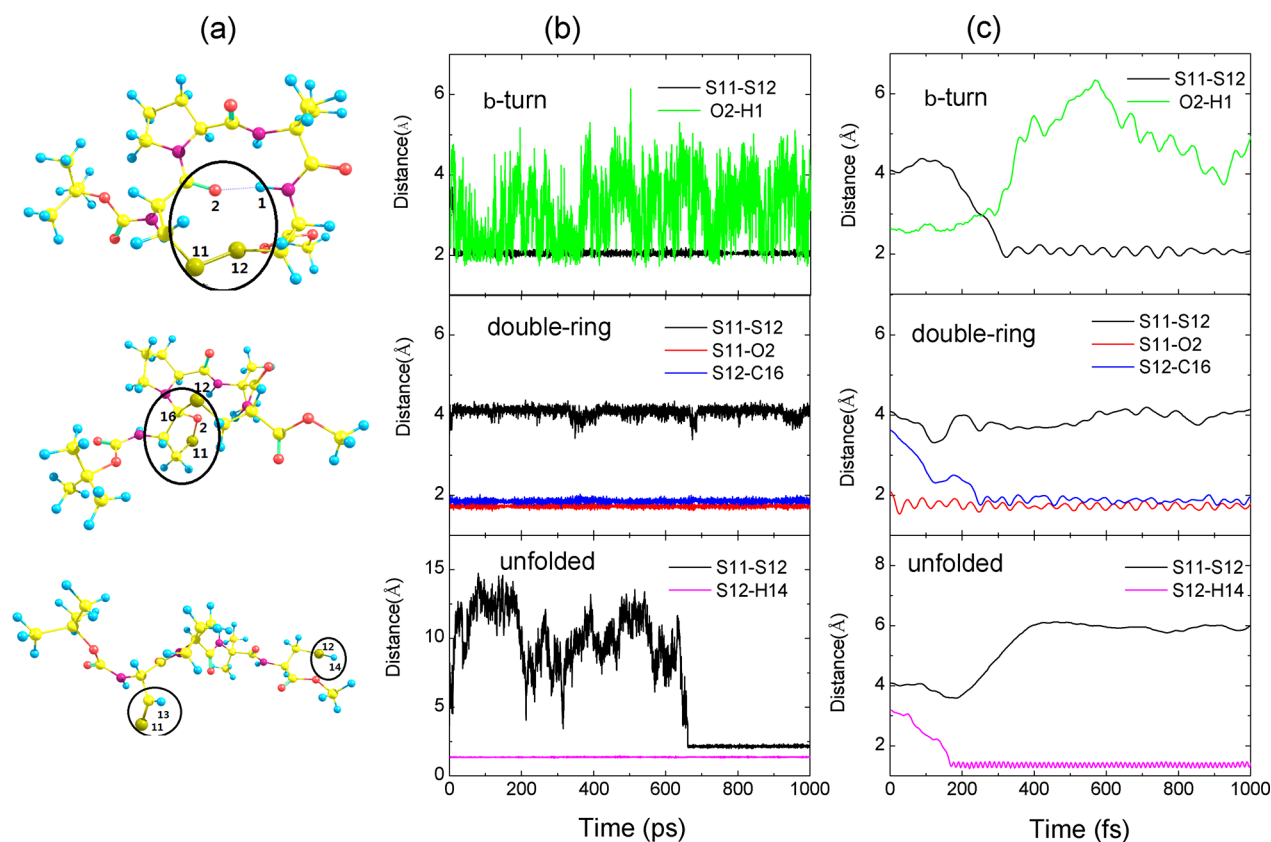


**Figure 2.** (a) Three typical conformations of the tetrapeptide after the photocleavage of the disulfide bridge in acetonitrile solvent molecules. (b) The time evolution of the conformation changes of the peptide characterized by specific bond distances on a long time scale of 1000 ps. (c) The time evolution of the conformation changes on a short time scale of 1000 fs.

linear response theory, it is written as the Fourier transform of the dipole moment time correlation function of the solute:<sup>20,21</sup>

$$I(\omega) = \frac{2\pi\beta\omega^2}{3cV} \int_{-\infty}^{\infty} dt \langle \mathbf{M}(t) \cdot \mathbf{M}(0) \rangle \exp(i\omega t) \quad (1)$$

where  $\beta = 1/kT$  with  $k$  being the Boltzmann constant and  $T$  the temperature.  $c$  is the speed of light in a vacuum.  $V$  is the volume of the system.  $M$  is the dipole moment of the solute. The angular bracket is the statistical average sampled by the MD simulation. In our simulations, the trajectories are recorded every 4 fs and terminated after 1 ns. Then, we assign the active bands to the vibrational modes by using the vibrational density of states (VDOS) formalism. It is obtained by the Fourier transformation of the atomic velocity autocorrelation function:<sup>21</sup>

$$\text{VDOS}(\omega) = \sum_{i=1}^N \int_{-\infty}^{\infty} dt \langle \mathbf{V}_i(t) \cdot \mathbf{V}_i(0) \rangle \exp(i\omega t) \quad (2)$$

where  $i$  runs over all of the atoms of the systems. The interpretation of the vibrational bands is done by decomposing the VDOS in terms of individual atomic motions. The interpretation of the spectra can also be done by Fourier transforming the autocorrelation function of the variation of the bond length.<sup>20</sup>

## RESULTS AND DISCUSSION

The potential energy profiles of the photoexcited tetrapeptide (in an acetonitrile solvent box) along the S–S bond fission for the ground  $S_0$  and excited  $S_{nc}(^1n\sigma^*)$  states are given in Figure

1b. Similar energy profiles in a methanol solvent box can be found in ref 11. When the S–S separation reaches 3.5 Å, the ground  $S_0$  and excited  $S_1$  surfaces intersect. At this conical intersection (CI) point, two cysteinyl radicals are generated. Starting from this CI point, we prepare 100 independent samples and carry out the combined PM6 semiempirical QM/MM MD simulation to simulate the conformational changes of the peptide.

Three typical conformation changes of the tetrapeptide in acetonitrile solvent are observed, as given in Figure 2a: (I) The cysteinyl radicals recombine quickly and the peptide refolds to the original  $\beta$ -turn architecture which is characterized by the intramolecular hydrogen bond formation between O2 and H1. (II) The peptide refolds to a double ring architecture which is characterized by the bond formations of S11–O2 and S12–C16. (III) The peptide unfolds to a fully opened state for several hundred picoseconds and recombines to the original  $\beta$ -turn architecture. The unfolded structure is characterized by the intramolecular hydrogen transfer of H13 (or H14) from C15 to S12.

Once the S–S bond is broken, the unsaturated cysteinyl radicals are not stable. They will either attract each other or be saturated by other intramolecular or intermolecular atoms. Our simulations show that 85% of the samples recombine to the original  $\beta$ -turn architecture in a short time. Figure 2b,c gives the S–S distance as a function of time for the three trajectories. We can see that the quick recombination event occurs on a time scale of 200 fs. This is in consistent with the ab initio MD (AIMD) simulation.<sup>12</sup> Our recent calculation<sup>11</sup> already found that 60% of the vibrational energy of the S–S bond relaxes to



the backbone of the peptide and solvent. The cysteinyl radicals could not get enough energy to power further unfolding. They recombine to their original architecture.

An interesting observation is that, for 10% of the samples, the peptide refolds to a double sulfur-heterocyclic ring structure. We notice that the cleavage of the S–S bond is accompanied by the hydrogen bond break between O2 and H1. Thereafter, the oxygen O2 may attract the vicinal S11 radical, resulting in a five-membered ring with the formation of the S11–O2 bond. At the same time, C16 forms a bond with the S12 radical, leading to another 11-membered ring; see Figure 2a. The S11–O2 and S12–C16 distances as a function of time in Figure 2b and c indicate that the intramolecular radical bicyclization reaction occurs in only 200 fs after the cleavage of the S–S bond. The refolded double ring architecture is very stable. No further unfolding of it has been observed in up to a few nanoseconds.

In other 5% trajectories, the S–S bond fully dissociates and approaches the maximum value of 15 Å in several hundred picoseconds. As pointed out above, when the S–S bond has been broken, S11 is attracted by O2. As a consequence, the intended motion of S11 may drive H13 (or H14) to move toward to S12 and form a hydrogen bond with it. Such hydrogen bonding is able to saturate the S12 radical and reduce the possibility of the radical bicyclization as well as the radical recombination. It in turn promotes the further separation of the S–S bond and leads to the final hydrogen transfer of H13 (or H14) onto S12. After the hydrogen transfer, S11 and C15 form double bonds. Figure 2b and c shows that H14 is transferred to S12 in only 200 fs. In contrast to the radical bicyclization reaction where the double ring architecture is stable in a few nanoseconds, the unfolded peptide via hydrogen transfer is metastable. Most of the unfolded samples recombine to their original  $\beta$ -turn architectures on a time scale of subnanoseconds. The mechanism of hydrogen transfer was suggested by H. Neiber et al. with the AIMD calculations.<sup>12</sup> However, in that work, the AIMD simulations were performed only for a small QM portion containing the S–S bridge and the  $C_\beta$  hydrogens of the solvated molecule on a time scale of 1 ps. The quantitative long lifetime of the S radicals on the electronic structure level of the whole peptide is unprecedentedly observed in our semiempirical QM/MM MD simulations.

The recombination of the S radicals, the radical bicyclization, and the intramolecular hydrogen transfer are competing processes resulting in different folding states of the peptide. In order to have a deep insight into the mechanisms governing the folding dynamics, we further compute the potential energy for the hydrogen transfer by using the CASPT2//CASSCF/Amber method; see Figure 1c. Our calculations show that, after the photocleavage of the S–S bond, the intramolecular hydrogen transfer from the Cys(1) group to S12 of the Cys(2) group is almost a barrier-free reaction (<5 kcal/mol). We also notice that the potential of the hydrogen-transferred state is 30 kcal/mol lower than the CI point but still 30 kcal/mol higher than the  $\beta$ -turn state. This can well explain the fact that the quantum yield of the fully unfolded structure is as low as 5% and its lifetime is on the scale of subnanoseconds. For the radical bicyclization, the reaction process is complicated. It is not easy to define the optimized reaction path to calculate the potential energy profile. Alternatively, the QM/MM minimum free-energy path (MFEP) method<sup>19</sup> should be used to study such a reaction. However, the computation of QM/MM MFEP

is expensive. We would like to report the result in a forthcoming work.

In methanol solvent, some different conformational changes of the tetrapeptide are observed, as already reported in our previous work.<sup>11</sup> Here we give a brief description for comparison: (I) We also obtain 85% samples with cysteinyl radical recombination. However, here the recombination occurs stochastically on a time scale from 10 ps (red line in Figure 3a)

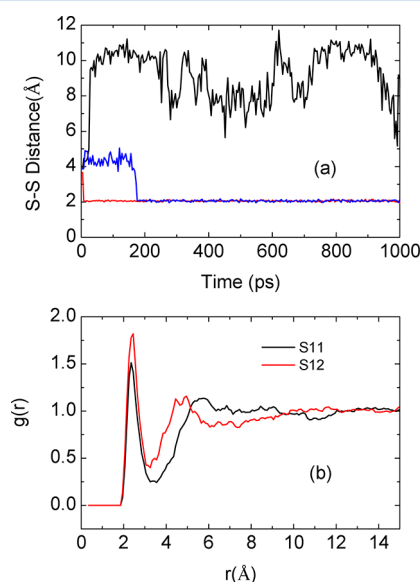


**Figure 3.** (a) Three examples of the time evolution of the S–S bond distance after the photocleavage for the peptide in methanol solvent molecules. (b) The radial distribution function  $g(r)$  between S radicals and the hydrogen H(O–CH<sub>3</sub>) of a methanol molecule as a function of the pair distance  $r$ .

to 200 ps (blue line in Figure 3a). (II) In another 15% of the samples, the peptides are fully opened and refold to the stable  $\alpha$ -helix structures characterized by the formation of an O6...H1 bond (black line in Figure 3a). The lifetime of the  $\alpha$ -helix architecture is longer than 1 ns. In contrast to the system with aprotic solvent of acetonitrile, for the peptide in the protic solvent of methanol, there is no intramolecular hydrogen transfer and radical bicyclization being observed. However, we find that the S radicals form hydrogen bonds with the polar solvent in all of the samples. The radial distribution function between S and H(O–CH<sub>3</sub>) in Figure 3b clearly indicates that the polar solvent forms cages around the two cysteinyl radicals. The saturation of the radicals prevents the recombination of the peptides. The different diffusion constants and polarities of the solvents might be other mechanisms that could affect the folding dynamics of the peptide. However, the diffusion constants of the acetonitrile and methanol obtained from our MD simulation are both close to  $2.5 \times 10^{-5}$  cm<sup>2</sup>/s. The polarity indexes of acetonitrile and methanol are 5.8 and 5.1, respectively, which are similar. For these two kinds of solvents, we propose that the caging effects due to the protic and aprotic natures are mainly responsible for the difference of the folding/unfolding dynamics of the tetrapeptide.

The peptide conformational changes are usually probed by the vibrational spectroscopy in experiment.<sup>9,10</sup> To find the relation between the microscopic 3D structure of the molecules and the experimental fingerprint, we compute the infrared spectra of the amide I mode of the tetrapeptide based on the

QM/MM MD simulations. Three typical IR spectra corresponding to the three typical architectures for the tetrapeptide in the acetonitrile solvent are presented in Figure 4. Each

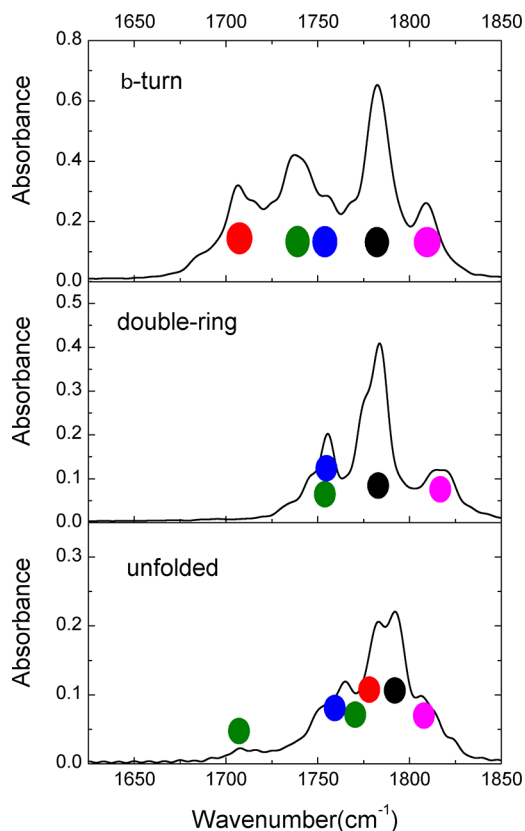


**Figure 4.** The calculated IR spectra in the amide I region of the tetrapeptide with three typical architectures in the acetonitrile solvent. The band assignments correspond to the colored C=O bonds in Figure 1a.

spectrum is produced by averaging the Fourier transform of the solute dipole autocorrelation function of all the samples having the same type of configurations. Please note that, for the peptide with unfolded structure, the Fourier transform does not include the trajectories after the recombination of the cysteinyl radicals. For the peptide in the  $\beta$ -turn forms, the spectrum has four well-resolved bands. The first band locating at  $1709\text{ cm}^{-1}$  is contributed by the  $\text{C16}=\text{O2}$  bond vibration; the second band at  $1739\text{ cm}^{-1}$  is assigned to  $\text{C5}=\text{O6}$  and  $\text{C9}=\text{O8}$  bonds. The other two bands correspond to the two C=O bonds outside of the turn. The relative band positions are consistent with the experimental observation.<sup>9,10</sup> The  $\text{C16}=\text{O2}$  vibrator excites the lower frequency mode because of the intramolecular hydrogen bond formation between O2 and H1 in the  $\beta$ -turn structure. For the peptide in the double ring form, the band at  $1709\text{ cm}^{-1}$  disappears due to the bond formations of  $\text{S11}-\text{O2}$  and  $\text{S12}-\text{C16}$  which quench the  $\text{C16}=\text{O2}$  vibration. For the peptide having the fully opened structure, the hydrogen bond between O2 and H1 breaks. An obvious blue shift of the band contributed by  $\text{C16}=\text{O2}$  is observed. Now the weak band at  $1709\text{ cm}^{-1}$  is contributed by  $\text{C5}=\text{O6}$  due to the weak hydrogen bond formation between O6 and H1.

The experimental transient IR spectra of the photocleaved tetrapeptide show that the spectral evaluation is characterized by three time constants.<sup>9,10</sup> In the early 20 ps, it represents a

red shift due to the heating of the molecule by the energy released after the cleavage of the S—S bond. Then, the amide I band with the lowest frequency presents a pronounced blue shift due to the intramolecular hydrogen bond weakening. It continues to grow on a 160 ps time scale. Then, the spectrum remains constant within 10  $\mu\text{s}$ . Kolano and his co-workers assigned such a finding to the strain in the peptide backbone that may keep the two S radicals apart and prevent recombination. Nieber et al. attributed the long lifetime of the S radicals to the intramolecular hydrogen transfer. However, our simulations show that the fully opened state caused by the intramolecular hydrogen transfer has a lifetime only on the scale of subnanoseconds. It cannot explain the constancy of the signal within microseconds. Alternatively, we found that the formation of the intramolecular  $\text{S11}-\text{O2}$  and  $\text{S12}-\text{C16}$  bonds well quenches the vibrational mode of the  $\text{C16}=\text{O2}$  bond at low frequency. Moreover, the double sulfur-heterocyclic ring structure with these two-bond formations is a stable state. We thus propose that the refolded double ring structure is responsible for the unchanged IR spectral shape in the long time scale.

## CONCLUSION

In conclusion, we have illustrated the unfolding and refolding dynamics of a photocleaved tetrapeptide with a disulfide bridge in acetonitrile and methanol solvents by using combined semiempirical QM/MM MD simulations. In the aprotic solvent of acetonitrile, the radical bicyclization reaction and intramolecular hydrogen transfer are responsible for the reduction of the recombination rate of the cysteinyl radicals. The peptide can refold/unfold to a double ring or a fully opened structure, respectively. In the protic solvent of methanol, the hydrogen bond formation between the polar solvent and the S radicals prolongs the lifetime of the cysteinyl radicals. The mechanisms of the recombination and hydrogen transfer are confirmed by the potential energy profiles obtained from high-levelled QM/MM calculations. Our calculated infrared spectra in the amide I region corresponding to the conformational changes of the peptide can well explain the experimental spectroscopy.

## AUTHOR INFORMATION

### Corresponding Author

\*E-mail: lhgao@bnu.edu.cn.

### Notes

The authors declare no competing financial interest.

## ACKNOWLEDGMENTS

This work is supported by the National Science Foundation of China (Grant No. 91127016) and the Major State Basic Research Development Programs (Grant No. 2011CB808503).

## REFERENCES

- (1) Dobson, C. M. *Nature* **2003**, 426, 884–890.
- (2) Lu, H. S. M.; Volk, M.; Kholodenko, Y.; Gooding, E. A.; Hochstrasser, R. M.; DeGrado, W. F. *J. Am. Chem. Soc.* **1997**, 119, 7173–7180.
- (3) Volk, M.; Kholodenko, Y.; Lu, H. S. M.; Gooding, E. A.; DeGrado, W. F.; Hochstrasser, R. M. *J. Phys. Chem. B* **1997**, 101, 8607–8616.
- (4) Volk, M. *Eur. J. Org. Chem.* **2001**, 2605–2621.
- (5) Schmidt, B.; Hogg, P. J. *BMC Struct. Biol.* **2007**, 7, 49–61.
- (6) Leeson, D. T.; Gai, F.; Rodriguez, H. M.; Gregoret, L. M.; Dyer, R. B. *Proc. Natl. Acad. Sci. U.S.A.* **2000**, 97, 2527–2532.

- (7) Lednev, I. K.; Karnoup, A. S.; Sparrow, M. C.; M. C. Asher, M. C. *J. Am. Chem. Soc.* **1999**, *121*, 4076–4077.
- (8) Chen, E.; P. Wittung-Stafshede, P.; Kliger, D. S. *J. Am. Chem. Soc.* **1999**, *121*, 3811–3817.
- (9) Kolano, C.; Helbing, J.; Kozinski, M.; Sander, W.; Hamm, P. *Nature* **2006**, *444*, 469–472.
- (10) Kolano, C.; Helbing, J.; Bucher, G.; Sander, W.; Hamm, P. *J. Phys. Chem. B* **2007**, *111*, 11297–11302.
- (11) Chen, X. B.; Gao, L. H.; Fang, W. H.; Phillips, D. L. *J. Phys. Chem. B* **2010**, *114*, 5206–5214.
- (12) Nieber, H.; Hellweg, A.; Dltsinis, N. L. *J. Am. Chem. Soc.* **2010**, *132*, 1778–1779.
- (13) Ferré, N.; Cembran, A.; Garavelli, M.; Olivucci, M. *Theor. Chem. Acc.* **2004**, *112*, 335–341.
- (14) Ponder, J.; Richards, W. F. M. *J. Comput. Chem.* **1987**, *8*, 1016–1024. See: <http://dasher.wustl.edu/ffe/>.
- (15) Wang, J.; Wang, W.; Kollman, P. A.; Case, D. A. *J. Comput. Chem.* **2005**, *25*, 1157–1174.
- (16) See: <http://www.gaussian.com/>.
- (17) See: <http://molcas.org/>.
- (18) Stewart, J. J. P. *J. Mol. Model.* **2007**, *13*, 1173–1213. See: <http://openmopac.net/>.
- (19) Hu, H.; Lu, Z. Y.; Yang, W. T. *J. Chem. Theory Comput.* **2007**, *3*, 390–406.
- (20) Yang, S.; Cho, M. *J. Chem. Phys.* **2005**, *123*, 134503–5.
- (21) Gaigeot, M.-P. *Phys. Chem. Chem. Phys.* **2010**, *12*, 3336–3359.